arXiv:1412.4348v1 [quant-ph] 14 Dec 2014

Nonclassical properties of Hermite polynomial's excitation on squeezed vacuum and its decoherence in phase-sensitive reservoirs

Shi-You Liu[1], Ya-Zhou Li[1],Li-Yun Hu[1,2*],Jie-Hui Huang[1,2], Xue-Xiang Xu[1], and Xiang-Yang Tao[1]
[1]*Center for Quantum Science and Technology, Jiangxi Normal University, Nanchang 330022, China and*
[2]*Beijing Computational Science Research Center, Beijing, 100084, China*

We introduce Hermite polynomial excitation squeezed vacuum (SV) $H_n(\hat{O})S(r)|0\rangle$ with $\hat{O} = \mu a + \nu a^\dagger$. We investigate analytically the nonclassical properties according to Mandel's Q parameter, second correlation function, squeezing effect and the negativity of Wigner function (WF). It is found that all these nonclassicalities can be enhanced by $H_n(\hat{O})$operation and adjustable parameters $\mu$and ν. In particular, the optimal negative volume $\delta_{opt}$of WF can be achieved by modulating $\mu$and ν for $n \geqslant 2$,while δ is kept unchanged for $n = 1$. Furthermore, the decoherence effect of phase-sensitive enviornment on this state is examined. It is shown that δ with bigger $n$diminishes more quickly than that with lower n, which indicates that single-photon subtraction SV presents more roboustness. Parameter $M$of reservoirs can be effectively used to improve the nonclassicality.

Keywords: completeness of representation, IWOP method, single- and two-variable Hermite polynomials

PACS: 03.65 -a. 42.50.Dv

I. INTRODUCTION

Nonclassical light fields play a critical rule in quantum optics and quantum information process [1]. Generation and manipulation of these states have attracted much attention to obtain a more effective quantum processing, such as teleportation, dense coding and quantum cloning. There are many schemes proposed to realize this purpose. Non-Gaussian operation, say photon addition and photon subtraction, has been widely employed to enhance the nonclassical properties of the input states [2–14]. For instance, a quantum-to-classical transition has been realized experimentally through single-photon–added coherent states of light [15]. For any photon–addition coherent state in the dissipative channel, its nonclassical properties are examined theoretically [16] by the analytical expression of the Wigner function (a Laguerre–Gaussian function). As another example, photon subtraction or addition has been used to improve entanglement between Gaussian states and the average fidelity of quantum teleportation [17, 18].

On the other hand, superposition of operators, such as $a^\dagger a$, $ta^\dagger + ra$, $a^2 + b^2$, $a^{\dagger 2} + b^{\dagger 2}$, are also applied to generate nonclassical states [19–24]. For example, the $ta^\dagger + ra$ operator is uesed to realize quantum state engineering and improve quantum entanglement or non-Gaussian entanglement distillation or the effect of quantum teleportation [19, 20]. In addition, this superposition operation is employed to enhance the degree of entanglement of even entangled coherent state [25]. Thus it will be interesting to investigate the different combination of elementary non-Gaussian operations to manipulate nonclassical quantum states. As a kind of polynomials states, for instace, the squeezed Hermoite states is found to be the minimum uncertain states for amplitude-squared squeezing [26]. In addition, the squeezed two-variable Hermite polynomial state is shown to be the minimum uncertain states for amplitude-squared squeezing, which is called as the sum-frequency squeezing states [27].

Recently, the Hermite polynomial's coherent state $H_n(Q)|\alpha\rangle$ is introduced [28], where $Q = (a + a^\dagger)/\sqrt{2}$ is the coordinate operator and $|\alpha\rangle = \exp\{\alpha a^\dagger - \alpha^* a\}|0\rangle$ is the Glauber coherent state. Then some nonclassical properties are discussed in details. In this paper, we shall introduce another kind of non-Gaussian state, which can be generated by operating Hermite polynomial of superposition of coherent photon-subtraction and addition (HPS), i.e., $H_n\left(\mu a + \nu a^\dagger\right)$ on single-mode squeezed vacuum (SV) $S(r)|0\rangle$. Single photon subtraction/addition SV, Hermite polynomial's subtraction $H_n(\mu a)$ and addition $H_n\left(\nu a^\dagger\right)$ SV can be considered as special cases of the HPS. It is interesting to notice that the HPS-SV can be generated by superposing some photon-addition and photon-subtraction SVs. As far as we know, there is no report in literature before.

This paper is arranged as follows. In section 2, we shall derive the normalization factor N_{μ_1,ν_1} for the non-Gaussian states. It is shown that N_{μ_1,ν_1} is just the Legendra polynomials, which is needed for clearly discussing the statistical properties of the HPS-SV. In section 3, we shall discuss nonclassical properties of the HPS-VS by ananlytically deriving Mandel's Q parameter, second correlation function, photon-number distribution, squeezing effect. In section 4, the Wigner function (WF) of the HPS-SV is obtained by using the property of Weyl ordered operators' invariance under similar transformations. In particular, the nonclassical property is presented according to the negativity of the WF. Section 5 is devoted to considering the effect of phase-sensitive reservoirs on the HPS-SV in terms of the negativity of WF. The last section is used to draw a conclusion.

II. THE HPS-SV AND ITS NORMALIZATION

The HPS-SV can be generated by operating Hemite polynomial operator $H_n\left(\mu a + \nu a^\dagger\right)$ on single-mode

squeezed vacuum $S(r)|0\rangle$,

$$|\Psi\rangle_H = N_{\mu_1,\nu_1} H_n(\hat{O}) S(r)|0\rangle, \hat{O} \equiv \mu a + \nu a^\dagger, \quad (1)$$

where N_{μ_1,ν_1} is the normailzarion factor to be determined, and $S(r) = \exp\{\frac{r}{2}(a^2 - a^{\dagger 2})\}$ is the squeezing operator with r being squeezing parameter, and $H_n(x)$ is the single-variable Hermite polynomials. a and $a^\dagger$ are the Bose anahilate and creation operator, respectively, satisfying communicative relation $[a, a^\dagger] = 1$.

In order to calculate N_{μ_1,ν_1}, using the transformation relation of single-mode squeezed operator [29], $S^\dagger(r) a S(r) = a\cosh r - a^\dagger \sinh r$, $S^\dagger(r) a^\dagger S(r) = a^\dagger \cosh r - a \sinh r$, we can get

$$S^\dagger(r) H_n(\hat{O}) S(r) = H_n(\hat{O}_1), (\hat{O}_1 \equiv \mu_1 a + \nu_1 a^\dagger), \quad (2)$$

where $\mu_1 = \mu\cosh r - \nu \sinh r$, $\nu_1 = \nu \cosh r - \mu \sinh r$. Thus the factor N_{μ_1,ν_1} can be calculated according to the normalization $1 = \langle\Psi|\Psi\rangle_H$, i.e.,

$$N_{\mu_1,\nu_1}^{-2} = \langle 0| H_n(\hat{O}_1^\dagger) H_n(\hat{O}_1)|0\rangle. \quad (3)$$

Then further employing the generating of function of single-variable Hermite polynomial,

$$H_n(x) = \left.\frac{\partial^n}{\partial t^n} e^{-t^2+2tx}\right|_{t=0}, \quad (4)$$

and the following operator identity [29] $e^{A+B} = e^A e^B e^{-\frac{1}{2}[A,B]} = e^B e^A e^{\frac{1}{2}[A,B]}$, which is valid for $[A,[A,B]] = [B,[A,B]] = 0$, we can put Eq.(3) into the form

$$\begin{aligned} N_{\mu_1,\nu_1}^{-2} &= \left.\frac{\partial^{2n}}{\partial\tau^n \partial t^n} \exp\left\{-A\left(\tau^2 + t^2\right) + 4\nu_1^2 t\tau\right\}\right|_{\tau,t=0} \\ &= 2^n n! B^n P_n\left(2\nu_1^2/B\right), \end{aligned} \quad (5)$$

where $A = 1 - 2\mu_1\nu_1$, $B = \sqrt{4\nu_1^4 - A^2}$, P_n is the Legendre polynomial, and we have used the new formula [30]

$$\begin{aligned} &\left.\frac{\partial^{2m}}{\partial t^m \partial\tau^m} \exp\left(-t^2 - \tau^2 + \frac{2x\tau t}{\sqrt{x^2-1}}\right)\right|_{t,\tau=0} \\ &= \frac{2^m m!}{(x^2-1)^{m/2}} P_m(x), \end{aligned} \quad (6)$$

in the last step of Eq.(5). Eq.(5) is just the analytical expression of the normalization factor N_{μ_1,ν_1}^{-2}.

In particular, when $(\mu,\nu) = (1,0),(0,1)$, leading to $(\mu_1,\nu_1) = (\cosh r, -\sinh r)$, $(-\sinh r, \cosh r)$, and $B = \sqrt{1-2e^{2r}}$, $\sqrt{1+2e^{-2r}}$, thus Eq.(5) reduces to

$$N_{1,0}^{-2} = 2^n n!\left(\sqrt{1-2e^{2r}}\right)^n P_n\left(\frac{2\sinh^2 r}{\sqrt{1-2e^{2r}}}\right), \quad (7)$$

$$N_{0,1}^{-2} = 2^n n!\left(\sqrt{1+2e^{-2r}}\right)^n P_n\left(\frac{2\cosh^2 r}{\sqrt{1+2e^{-2r}}}\right), \quad (8)$$

which are just the normalization factors of Hermite subtraction and Hermite addition squeezed vacuum, respectively. In addition, when the squeezing parameter $r = 0$ leading to $\mu_1 = \mu$, $\nu_1 = \nu$, i.e., the HPS vacuum ($|\Psi\rangle_{HPS} \to |\Psi\rangle$), we see

$$|\Psi\rangle \equiv N_{\mu,\nu} H_n(\hat{O})|0\rangle, \; N_{\mu,\nu}^{-2} = \left\{N_{\mu_1,\nu_1}^{-2}\right\}_{(\mu_1,\nu_1)\to(\mu,\nu)}. \quad (9)$$

In the state, we can get the average

$$\left\langle a^{\dagger l} a^k\right\rangle = \frac{N_{\mu,\nu}^2 \nu^{2n} (2\lambda)^{l+k} (n!)^2}{\lambda^{2n}(n-l)!(n-k)!} F_{n-l,n-k}\left(\lambda^2\right), \quad (10)$$

where $\lambda = \nu/\sqrt{1-2\mu\nu}$ and we have define a special function whose mother function is given by

$$F_{m,n}\left(\lambda^2\right) \equiv \left.\frac{\partial^m}{\partial s^m}\frac{\partial^n}{\partial t^n} e^{-t^2-s^2+4st\lambda^2}\right|_{s=t=0}. \quad (11)$$

From Eq.(10) one can see that $\left\langle a^{\dagger l} a^k\right\rangle = \left\langle a^{\dagger k} a^l\right\rangle^*$, $\left\langle a^{\dagger l}\right\rangle = \left\langle a^l\right\rangle^*$ and $\langle a\rangle = 0$, as expected. In particular, when $k = l$, Eq.(10) reduces to

$$\begin{aligned} \left\langle a^{\dagger l} a^l\right\rangle &= \frac{2^{n+l} N_{\mu,\nu}^2 (n!)^2}{(n-l)!} v^{2l} K^{(n-l)/2} P_{n-l}\left(\frac{2\nu^2}{\sqrt{K}}\right) \quad (12) \\ &(K = 4\nu^4 - (1-2\mu\nu)^2, n \geqslant l), \end{aligned}$$

Eq.(10) shall be useful for further calculations.

III. NONCLASSICAL PROPERTIES OF THE HPS-VS

In this section, we study the nonclassical properties of the HPS-VS according to Mandel's Q parameter, photon-number distribution, and squeezing effect.

A. Mandel's Q parameter and second-order correlation function

We examine the sub-Poissonian photon statistics by using Mandel's Q parameter [31], which is defined as

$$Q_M = \frac{\left\langle a^{\dagger 2} a^2\right\rangle_H}{\left\langle a^\dagger a\right\rangle_H} - \left\langle a^\dagger a\right\rangle_H. \quad (13)$$

Super-Poissonian, Poissonian, and sub-Poissonian statistics correspond to $Q_M > 0$, $Q_M = 0$, and $Q_M < 0$,respectively. In order to obtain the result (13), it will be convinient to derive some average values: $\left\langle a^2\right\rangle$, $\left\langle a^4\right\rangle$, $\left\langle a^\dagger a\right\rangle$, $\left\langle a^{\dagger 3} a\right\rangle$ and $\left\langle a^{\dagger 2} a^2\right\rangle$ under the state $|\Psi\rangle$ (9). These averages are obtained from Eq.(10). Thus under the state $|\Psi\rangle_H$, these corresponding average values ($\langle ...\rangle_H = \left\{\left\langle S^\dagger ... S\right\rangle\right\}_{\mu\to\mu_1,\nu\to\nu_1}$) are given by

$$\begin{aligned} \left\langle a^\dagger a\right\rangle_H = \Big\{&\left\langle a^\dagger a\right\rangle \cosh 2r + \sinh^2 r \\ &- \frac{\sinh 2r}{2}\left\langle a^{\dagger 2} + a^2\right\rangle\Big\}_{\mu\to\mu_1,\nu\to\nu_1}, \end{aligned} \quad (14)$$

and

$$\begin{aligned}&\left\langle a^{\dagger 2}a^{2}\right\rangle_{H}\\&=\left\{\frac{1}{4}\left(3\cosh 4r+1\right)\left\langle a^{\dagger 2}a^{2}\right\rangle+\frac{1}{4}\left\langle a^{\dagger 4}+a^{4}\right\rangle\sinh^{2}2r\right.\\&+\left(\sinh 2r-\frac{3}{4}\sinh 4r\right)\left\langle a^{\dagger 2}+a^{2}\right\rangle\\&-\frac{1}{2}\left\langle a^{\dagger}a^{3}+a^{\dagger 3}a\right\rangle\sinh 4r+4\left\langle a^{\dagger}a\right\rangle\left(3\cosh^{2}r-1\right)\sinh^{2}r\\&\left.+(3\cosh^{2}r-2)\sinh^{2}r\right\}_{\mu,\nu\rightarrow\mu_{1},\nu_{1}}. \qquad (15)\end{aligned}$$

Substituting Eq.(10) into Eq.(13), we can get the Mandel's Q parameter. The second-order correlation function [32] $g^{(2)}=\left\langle a^{\dagger 2}a^{2}\right\rangle_{H}/\left\langle a^{\dagger}a\right\rangle_{H}^{2}$ can also be gotten by using Eqs.(14) and (16). In particular, when $n=0$ (corresponding to the squeezed vacuum), the Mandel's Q parameter and the second-order correlation function are given by $Q_M=\cosh 2r>1$, and $g^{(2)}=3+1/\sinh^{2}r>3$, respectively.

In order to clearly see the effects of Hermite polynomial on squeezed vacuum, the numerical calculation results of squeezing parameter r and Mandel's Q parameter Q_M, $g^{(2)}$ are plotted as the functions of squeezing parameter r in Figs.1, 2, respectively. From Fig.1(a) for a given (μ,ν)=$(1,1)$, it is easy to see that the HPS-SV presents a sub-Poissonian statistics (except for $n=0$) in a small region of parameter $r\lesssim 0.5$ and the value of Q_M increases with r. However, the absolute value of Q_M decreases with n in this region. For a given value of $n=2$, and several asymmetrical cases of (μ,ν), on one hand, from Fig.1(b) one can see that the negative feature can be enhanced by Hermite polymials addition $H_2(a^{\dagger})$ operation rather than Hermite polymials subtraction operator $H_2(a)$. The latter shows a similar trend to the SV due to their similar photon-number distributions. On the other hand, the asymmetrical coherent superposition of subtraction and addition (say, $H_2(a+9a^{\dagger})$) can be more effective for improving the negative feature of Q_M than $H_2(a)$ and $H_2(a+a^{\dagger})$. In addition, from Fig.2 one can get similar results for the second-order correlation function. For instance, the HPS-SV appears antibunching effect in a small region due to the Hermite operation (except for $n=0$).

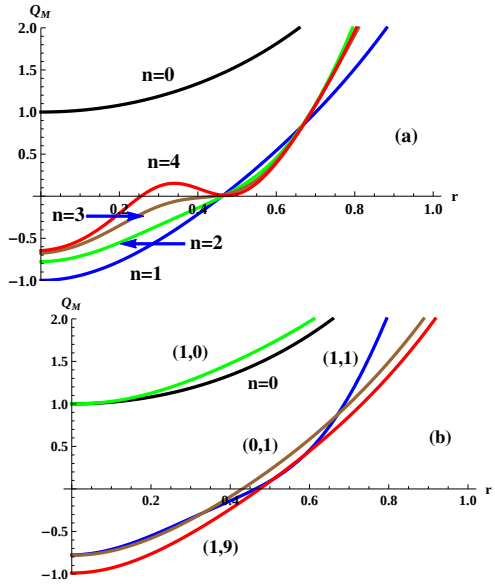

FIG. 1: (Color online) Mandel's Q parameter Q_M as a function of squeezing parameter r for several different values of n and (μ,ν). (a) (μ,ν)=$(1,1)$; (b) $n=2$.

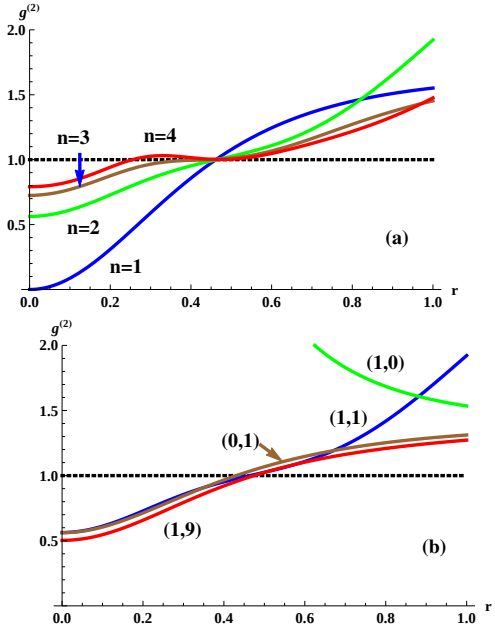

FIG. 2: (Color online) The second-order correlation function $g^{(2)}$ as the function of squeezing parameter r for several different values of n and (μ,ν). (a) (μ,ν)=$(1,1)$; (b) $n=2$.

B. Photon-number distribution

Now, we discuss the photon-number distribution of the HPS-SV. In this field, the photon-number distribution (PND) of finding m photons is given by $P_H=\left|N_{\mu_1,\nu_1}\left\langle m\right|H_n(\hat{O})S\left(r\right)\left|0\right\rangle\right|^2$. Employing the unnormalized coherent state $\left|\alpha\right\rangle=\exp[\alpha a^{\dagger}]\left|0\right\rangle$ ($\left\langle 0\right|\left.\alpha\right\rangle=1$) [33, 34], leading to $\left|m\right\rangle=\frac{1}{\sqrt{m!}}\frac{\mathrm{d}^m}{\mathrm{d}\alpha^m}\left|\alpha\right\rangle|_{\alpha=0}$, $\left(\left\langle\beta\right.\left|\alpha\right\rangle=e^{\alpha\beta^*}\right)$, and the SV [29, 32]

$$S\left(r\right)\left|0\right\rangle=\mathrm{sech}^{1/2}r\exp\left(-\frac{1}{2}a^{\dagger 2}\tanh r\right)\left|0\right\rangle, \qquad (16)$$

as well as Eq.(4) ($e^{\alpha a}a^{\dagger}e^{-\alpha a}=a^{\dagger}+\alpha$), we have

$$\begin{aligned}&\langle m|\,H_n(\hat{O})S\left(r\right)|0\rangle\\&=\frac{\mathrm{sech}^{1/2}r}{\sqrt{m!}}\,\frac{\partial^m\partial^n}{\partial\alpha^{*m}\partial t^n}e^{-A_1^2t^2-B_1^2\alpha^{*2}+2t\alpha^*C_1}\Big|_{t=\alpha^*=0},\end{aligned}\tag{17}$$

where we have set $A_1^2=1+2\mu^2\tanh r-2\mu\nu$, $B_1^2=\frac{1}{2}\tanh r$, $C_1=\nu-\mu\tanh r$. Thus the photon-number distribution is

$$\begin{aligned}P_H\left(m\right)&=N_{\mu_1,\nu_1}^2m!\left(n!\right)^2\mathrm{sech}r\\&\times\left|\frac{\partial^m\partial^n}{\partial\alpha^{*m}\partial t^n}e^{-A_1^2t^2-B_1^2\alpha^{*2}+2t\alpha^*C_1}\Big|_{t=\alpha^*=0}\right|^2,\end{aligned}\tag{18}$$

which is the PND of the HPS-SV. It is easy to see that Eq.(18) just reduces to the photon-number distribution of SV when $n=0$; while for $r=0$, (i.e., the Hermite polynomial vacuum state $H_n(\hat{O})\,|0\rangle$), the PND is given by

$$\begin{aligned}P_H\left(m\right)&=N_{\mu,\nu}^2m!\left(n!\right)^2\\&\times\left|\sum_{l=0}^{[n/2]}\frac{\left(2\mu\nu-1\right)^l\left(2\nu\right)^{n-2l}}{l!\left(n-2l\right)!}\delta_{m,n-2l}\right|^2.\end{aligned}\tag{19}$$

In particular, when $m=n$, using the formula [30]

$$P_m\left(x\right)=x^m\sum_{l=0}^{[m/2]}\frac{m!}{2^{2l}l!l!(m-2l)!}\left(1-\frac{1}{x^2}\right)^l,\tag{20}$$

we have

$$\begin{aligned}&P_H\left(n\right)=N_{\mu,\nu}^2\left(n!\right)^2\,2^{2n}\mathrm{sech}r\left|\,D_1^{n/2}P_n\left(C_1/\sqrt{D_1}\right)\right|^2,\\&\left(D_1=C_1^2-A_1^2B_1^2\right).\end{aligned}\tag{21}$$

In Fig.3, the PND is poltted for different values (μ,ν), r and n, from which one can see that (i) by modulating the order of Hermite polynomials, one has able to change the position of peak [see Fig.3 (a) and (d)]; (ii) for a small squeezing (say $r=0.3$), the peak of PND is mainly located at n [see Fig. 3 (a), (b), (d)]; (iii) for a large squeezing (say $r=0.9$), the peak moves to the small photon-number region (see Fig.3(b)); (iv) in addition, the PND can also be modulated by the parameters [see Fig.3 (a) and (c)], expecially for $n\geqslant 2$.

C. Squeezing effects

In this subsection, we consider the squeezing effects of the HPS-SV, eapecially from the Hermite polynomial operation. First, we examine the wave function which can reflect the the squeezing effect of quantum state

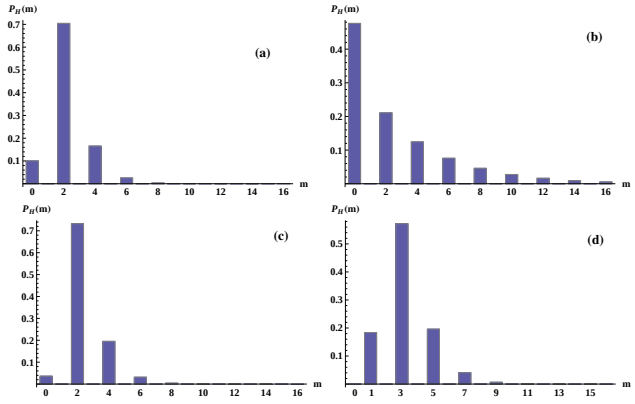

FIG. 3: (Color online) The photon-number of the HPS-SV distribution as a function of m for several different parameters r, n and (μ,ν). (a) $n=2, r=0.3$, $\mu,\nu=1/\sqrt{2}$; (b) $n=2, r=0.9$, $\mu,\nu=1/\sqrt{2}$; (c) $n=2, r=0.3$, $\mu=1,\nu=3$; (d) $n=3, r=0.3$, $\mu,\nu=1/\sqrt{2}$.

to some extent. Using the natural expression of single-mode squeezing operator in the momentum representation $|p\rangle$ [35],

$$S\left(r\right)=\sqrt{u}\int_{-\infty}^{\infty}dp\,|up\rangle\,\langle p|\,,u=e^r,\tag{22}$$

which leads to $S^{\dagger}\left(r\right)|p\rangle=1/\sqrt{u}\,|p/u\rangle$, thus the wave function can be derived as

$$\begin{aligned}\Psi_H\left(p\right)&=\langle p|\,\Psi\rangle_H=N_{\mu,\nu}\,\langle p|\,SS^{\dagger}H_n\left(\hat{O}\right)S\,|0\rangle\\&=\frac{N_{\mu,\nu}}{\sqrt{u}}\left\langle\frac{p}{u}\right|H_n\left(\hat{O}_1\right)|0\rangle\,.\end{aligned}\tag{23}$$

Now we calculate the matrix element $\langle p|\,H_n(\hat{O})\,|0\rangle$. Using the normal ordering form of $H_n(\hat{O})$ and Eq.(4), ($e^{\alpha a}a^{\dagger}e^{-\alpha a}=a^{\dagger}+\alpha$), and noticing that [35] $|p\rangle=\pi^{-1/4}\exp\{-\frac{1}{2}p^2+\sqrt{2}ipa^{\dagger}+\frac{1}{2}a^{\dagger 2}\}\,|0\rangle$, we have ($\lambda=\nu/\sqrt{1-2\mu\nu}$)

$$\begin{aligned}&\langle p|\,H_n\left(\hat{O}\right)|0\rangle\\&=\frac{1}{\pi^{1/4}}\left(\sqrt{1-2\lambda^2}\frac{\nu}{\lambda}\right)^n e^{-\frac{1}{2}p^2}H_n\left(\frac{-i\sqrt{2}\lambda p}{\sqrt{1-2\lambda^2}}\right).\end{aligned}\tag{24}$$

Thus the distribution of the quadrature p is given by

$$\begin{aligned}\left|\Psi_H\left(p\right)\right|^2&=\frac{N_{\mu,\nu}^2}{\pi^{1/2}u}e^{-u^{-2}p^2}\left|1-2\mu_1\nu_1-2\nu_1^2\right|^n\\&\times\left|H_n\left(\frac{-i\sqrt{2}\nu_1p/u}{\sqrt{1-2\mu_1\nu_1-2v_1^2}}\right)\right|^2,\end{aligned}\tag{25}$$

where $(u=e^r)$ and μ_1,ν_1 are defined above. Eq.(25) is just the Hermite-Gaussian function.

In order to clearly see the squeezing effect, we present the distribution in Fig.4 where the distributions are plotted for different values of n and (μ,ν). Different from

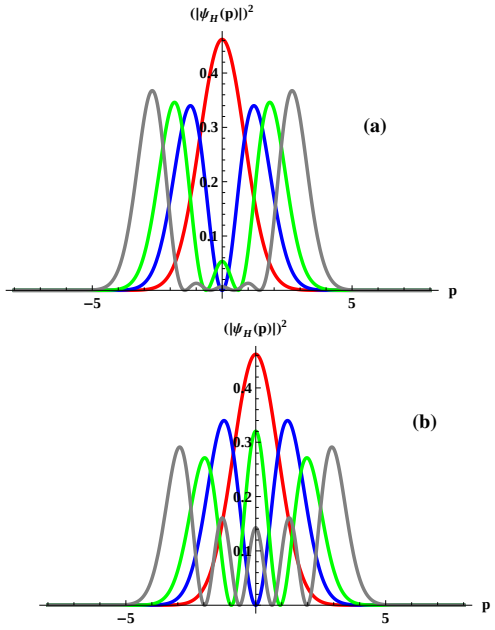

FIG. 4: (Color online) The distributions of the quadrature p of the HPS-SV as a function of p for several different parameters n and (μ,ν) with $r=0.2$. Red, Blue, Green and Gray lines correspond to $n=0,1,2,4$, respectively. (a) $\mu=\nu=1/\sqrt{2}$;(b) n=1,2,4 correspond to $(\mu,\nu)=(0,1)$, $(1,2)$, $(1,6)$, respectively.

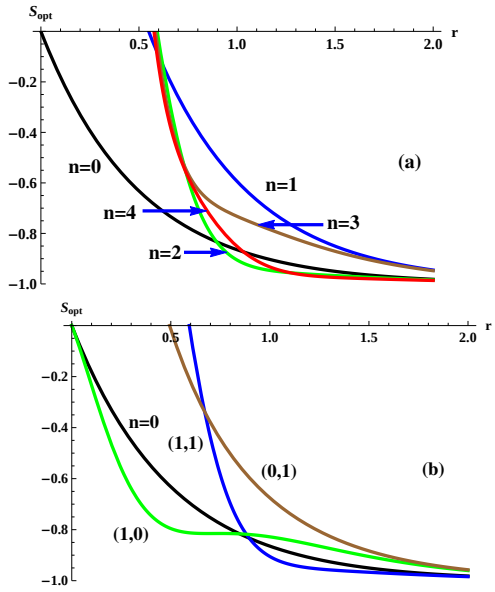

FIG. 5: (Color online) The degree of squeezing S_{opt} of HPS-SV as the function of squeezing parameter r for several different values of n and (μ,ν). (a) (μ,ν)=$(1,1)$; (b) $n=2$.

the Gaussian distribution of squeezed state (n=0), the HPS-SV has several different peak distributions with different $n(\neq 0)$ values. In addition, the amplitude values of peaks affected by the parameters μ,ν (see Fig.4(b)).

Next, we further discuss the squeezing property of the HPS-SV by using the standard analysis of quadrature squeezing, i.e., $(\triangle Q)^2<1$ or $(\triangle P)^2<1$ which indicates the squeezing or sub-Poissonian statistics. Here, we introduce a quadrature operator $Q_\theta=ae^{-i\theta}+a^\dagger e^{i\theta}$. Thus the squeezing can be characterized by the minimum value $\langle\triangle^2 Q_\theta\rangle<1$ with respect to θ, or by the normal ordering form $\langle:\triangle^2 Q_\theta:\rangle<0$ [36]. Upon expanding the terms of $\langle:\triangle^2 Q_\theta:\rangle$, one can minimize its value over the whole angle θ, which is given by [37] $S_{opt}=-2\left|\langle a^{\dagger 2}\rangle-\langle a^\dagger\rangle^2\right|+2\langle a^\dagger a\rangle-2\left|\langle a^\dagger\rangle\right|^2$, then its negative value in the range $[-1,\,0)$ indicates squeezing (or nonclassical). For the HPS-SV, $\langle a^\dagger\rangle=0$, using Eq.(14), the degree of squeezing of the HPS-SV can be obtained

$$S_{HPS}=2\left\{\langle a^\dagger a\rangle_H-\left|\langle a^{\dagger 2}\rangle_H\right|\right\}<0, \qquad (26)$$

which indicates that the negative value of S_{HPS} only emerges when $\langle a^\dagger a\rangle_H<\left|\langle a^{\dagger 2}\rangle_H\right|$, where $\langle a^2\rangle_H=\langle a^2\cosh^2 r+a^{\dagger 2}\sinh^2 r-a^\dagger a\sinh 2r\rangle_{\mu\to\mu_1,\nu\to\nu_1}$-$\frac{1}{2}\sinh 2r$. In particular, when $n=0$ (i.e., the case of squeezed vacuum), $S_{HPS}=-2e^{-r}\sinh r$, as expected.

The degree of squeezing of the HPS-SV is shown in Fig. 5 for several different values of parameters n and (μ,ν). It is found that the degree of squeezing of the HPS-SV increases with r. In Fig.5 (a) with a given (μ,ν)=(1,1), comparing with the SV (n=0), the HPS-SV can present squeezing only when the squeezing parameter r exceeds a certain threshold value (say 0.5); the degree of squeezing can be enhanced by Hermite polynomials superposition operation (say $n=2,4$) in a larger region of squeezing parameter. In Fig.5 (b) with $n=2$, it is shown that (i) the Hermite photon-subtraction operation $H_2(a)$ on the SV can be used to improve the degree of squeezing in a small region ($r\lesssim 0.6$), while for $H_2(a^\dagger)$ the case is not true; the coherent superposition operation ($H_2(a+a^\dagger)$), rather than the $H_2(a)$ or $H_2(a^\dagger)$ operations, can improve the degree of squeezing in a large region. This implies that the coherent operation $\mu a+\nu a^\dagger$ achieves better squeezing than the mere photon-subtraction (-addition) in a large region of r. In addition, the maximum degree of squeezing of the HPS-SV is -1.

IV. WIGNER DISTRIBUTION OF THE HPS-SV

As a kind of quasi-probability function, the Wigner function (WF) is a powerful tool to describe the nonclassicality of optical fields, whose partial negativity implies the highly nonclassical properties of quantum states. In addition, the negativity is often used to present the decoherence of quantum states. In this section, we derive the analytical expression of WF for the HPS-SV by using the the Weyl ordered operators' invariance under similar

transformations [38]. For a single-mode quantum system, the WF can be calculated as $W = \mathrm{tr}[\rho\Delta(\alpha)]$, where $\Delta(\alpha)$ single-mode Wigner operator [38, 39],

$$\Delta(\alpha) = \frac{e^{2|\alpha|^2}}{\pi}\int\frac{d^2\beta}{\pi}|\beta\rangle\langle-\beta|e^{2(\alpha\beta^*-\alpha^*\beta)} = \frac{1}{2}\vdots\,\delta(\alpha-a)\,\delta\left(\alpha^*-a^\dagger\right)\vdots. \quad (27)$$

Here $\alpha = (q+ip)/\sqrt{2}$ and the symbol $\vdots\ \vdots$ denotes Weyl ordering.

The merit of Weyl ordering lies in the Weyl ordered operators' invariance under similar transformations proved, which means $S\vdots(\circ\circ\circ)\vdots S^{-1} = \vdots S(\circ\circ\circ)S^{-1}\vdots$, as if the "fence" $\vdots\ \vdots$ did not exist, so S can pass through it. Then following this invariance and the above squeezing transform relations, we have

$$S^\dagger\Delta(\alpha)S = \frac{1}{2}\vdots\,\delta(\bar{\alpha}-a)\,\delta\left(\bar{\alpha}^*-a^\dagger\right)\vdots = \Delta(\bar{\alpha}), \quad (28)$$

where $\bar{\alpha} = \alpha\cosh r + \alpha^*\sinh r$. Thus the WF can be derived

$$W(\alpha,\alpha^*) = N_{\mu_1,\nu_1}^2\langle 0|H_n\left(\hat{O}_1^\dagger\right)\Delta(\bar{\alpha})H_n\left(\hat{O}_1\right)|0\rangle. \quad (29)$$

Further employing Eq.(4) we can obtain

$$\begin{aligned} W(\alpha,\alpha^*) &= \frac{e^{-2|\bar{\alpha}|^2}}{\pi N_{\mu_1,\nu_1}^{-2}}\frac{\partial^{2n}}{\partial\tau^n\partial t^n} \\ &\times e^{4\nu_1\bar{\alpha}\tau+4\nu_1\bar{\alpha}^*t-4\nu_1^2t\tau+(2\mu_1\nu_1-1)\left(\tau^2+t^2\right)}\Big|_{\tau=t=0} \\ &= \frac{1}{\pi}\sum_{l=0}^{n}\frac{(n!)^2\left(-4\nu_1^2\right)^l(2\mu_1\nu_1-1)^{n-l}}{l!\left[(n-l)!\right]^2N_{\mu,\nu}^{-2}e^{2|\bar{\alpha}|^2}} \\ &\times\left|H_{n-l}\left(\frac{2\nu_1\bar{\alpha}}{i\sqrt{2\mu_1\nu_1-1}}\right)\right|^2. \end{aligned} \quad (30)$$

Obviously, the WF $W(\alpha,\alpha^*)$ in Eq.(30) is a real function and is non-Gaussian in phase space due to the presence of $H_{n-l}(x)$. In particular, when $n=0$, Eq.(30) just reduces to the WF of the squeezed vacuum, $\frac{1}{\pi}e^{-2|\alpha\cosh r+\alpha^*\cosh r|^2}$, as expected. In addition, when $n=1$ corresponding to the single photon-subtraction (-addition) squeezed vacuum, ($H_0(x)=1, H_1(x)=2x$)

$$W(\alpha,\alpha^*) = \frac{e^{-2|\bar{\alpha}|^2}}{\pi}\left(4|\bar{\alpha}|^2-1\right), \quad (31)$$

which indicates that there is always negative region at the center of phase space $\alpha=0$ (independent of the two parameters μ,ν). In Fig.6, the Wigner distributions are depicted in phase space for several different parameter values n, and (μ,ν), from which it clearly see that there are some obvious negative regions of the WF in the phase space which is an indicator of the nonclassicality of the state. In addition, these negative areas are modulated not only by n [see Fig.6 (a)-(c)], but also by the parameters (μ,ν) [see Fig.6 (b) and (d)]. For instance, there

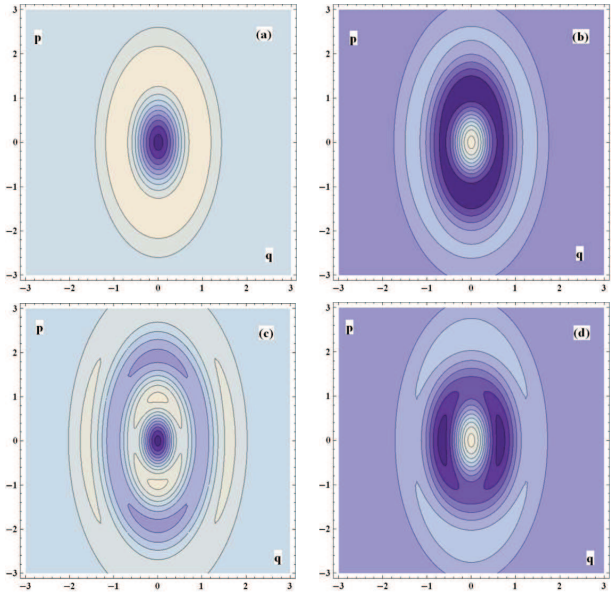

FIG. 6: (Color online) Contour plot of the Wigner function after the Hermite polynomials coherent operation on the SV with $r=0.3$ for several different n and (μ,ν). (a) $n=1$; (b) $n=2$, $\mu,\nu=1$; (c) $n=3$, $\mu,\nu=1$; (d) $n=2$, $\mu=1$, $\nu=9$, where only the negative regions are colored in blue.

is obvious difference of WF distribution between Fig.6 (b) and (d). That is to say, for higher order case $n\geqslant 2$, the negative area depends on the two parameters. In order to clearly see this point, we can quanlify the negative volume of the WF, defined by $\delta = \frac{1}{2}[\int_{-\infty}^{\infty}dqdp\,|W(q,p)|\text{-}1]$ [40].

In Fig. 7, the negative volume of WF as a function of r or ν on applying the Hermite coherent suposition operatopn $H_n(\mu a+\nu a^\dagger)$ for several different n. From Fig.7(a), one can find that the negative volume δ increases with the order n (in a certain region of $r\lesssim 0.45$) and decreases with r. In particular, for the case of $n=1$ (corresponding to a superposition between single-photon addition/subtraction SV and SV), the negative volume is independent of parameters r and (μ,ν) and is kept unchanged ($\delta=0.2131$). In fact, using Eq.(31) one can calculate that the negative volume of WF with $n=1$ is $\delta = 2/\sqrt{e}-1\approx 0.2131$. In Fig.7(b), we optimize the negative volume for different r and n, where μ,ν are taken as $\mu=\sqrt{1-\nu^2}$. From Fig.7(b), it is found that (i) when $\mu=\nu=1/\sqrt{2}$, the negative volume δ increases with the order n for a given small r and decreases with r for a given n (see the vertical dotted line at the point of $\nu=1/\sqrt{2}$); (ii) for a given parameter $r=0.1$, the negative volume δ increases with n when ν exceeds a certain threshold ($\nu\approx 0.41$); (iii) for a given $n=2$, δ decreases with r when ν exceeds a certain threshold ($\nu\approx 0.45$); (iv) the negative volume δ does not monotonously increase with ν; in particular, one can find the maximum negative volume δ in a bigger region of ν ($\nu\geqslant 0.41$) for $n=2,3,4$. This optimal value of δ can be achieved

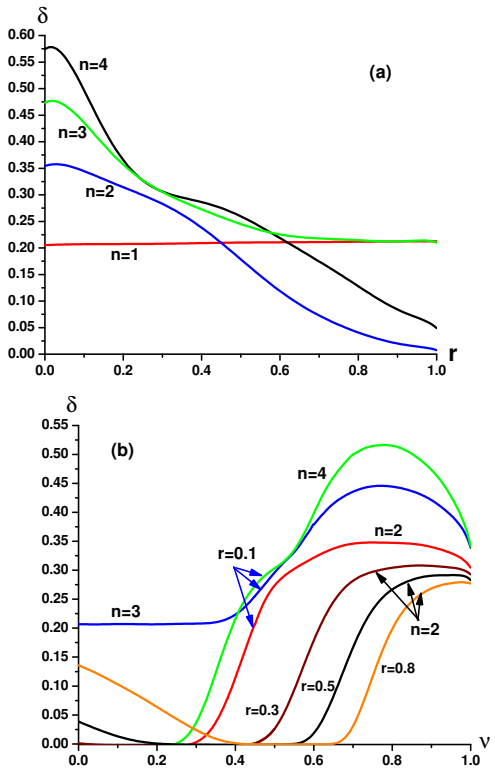

FIG. 7: (Color online) Negative volume of the Wigner function as a function of (a) squeezing parameter r, and μ=ν=$1/\sqrt{2}$; (b) parameter ν with $\mu=\sqrt{1-\nu^2}$ for several different $n=1,2,3,4$, and $r=0.1,0.3,0.5,0.8$.

at neither $\nu=0$ nor $\nu=1$. For instance, this points are $\nu\approx 0.71, 0.74, 0.78$ for different values of $n=2,3,4$ and $r=0.1$. These indicate that the effects of the coherent operation $H_n(\mu a+\nu a^\dagger)$ with higher order $n\geqslant 2$ are prominent than those of the mere photon subtraction $H_n(\nu a^\dagger)$ and the addition $H_n(\nu a^\dagger)$ particularly in the larger region of parameter ν, whereas the optimal operation is not the photon subtraction or the photon addition in this region. This result is different from that in Ref.[19].

V. DECOHERENCE OF THE HPS-SV IN PHASE-SENSITIVE RESERVOIRS

In this section, we shall examine the time evolution of the HPS-SV at the presence of phase-sensitive reservoirs. In the interaction picture and the Born and Markow approximation, the time evolution of the density matrix is governed by the master equation (ME) [41]:

$$\frac{d}{dt}\rho(t)=\kappa\bar{n}L\left[a^\dagger\right]\rho+\kappa\left(\bar{n}+1\right)L\left[a\right]\rho + \kappa MD\left[a\right]\rho+\kappa M^*D\left[a^\dagger\right]\rho, \tag{32}$$

and

$$L\left[O^\dagger\right]\rho=2O^\dagger\rho O-OO^\dagger\rho-\rho OO^\dagger, \tag{33}$$

$$D\left[a\right]\rho=2a^\dagger\rho a^\dagger-a^{\dagger 2}\rho-\rho a^{\dagger 2}. \tag{34}$$

where κ and $\bar{n}$ are the dissipative coefficient and the average thermal photon number of the environment, respectively. Here M is the complex correlation parameter between modes symmetrically displaced about center frequency. In fact, the ME in Eq.(32) includes two special cases: (1) For an uncorrelated reservoir, i.e., $M=0$, Eq.(32) becomes the ME describing the interaction between a system and a thermal environment at finite temperature; (2) when $M=\bar{n}=0$, Eq.(32) reducess to the one describing the photon-loss channel. For an (non)ideally squeezed reservoir, the constraint condition $|M|^2=\bar{n}\left(\bar{n}+1\right)$ ($|M|^2<\bar{n}\left(\bar{n}+1\right)$) is required.

In Ref.[42], we derived the Kraus operator-sum representation of density operator ρ and the time evolution of some distibution functions by using the thermal entangled state representation $\langle\eta|$. The evolution of Wigner function is given by

$$W(\alpha,t)=\frac{2\mu_\infty}{T}\int\frac{d^2\beta}{\pi}e^{-\frac{2\mu_\infty^2}{T}\Sigma(\bar{\alpha},\bar{\alpha}^*)}W(\beta,0), \tag{35}$$

where $T=1-e^{-2\kappa t}$, $\bar{\alpha}=\alpha-\beta e^{-\kappa t}$, and $\mu_\infty=1/\sqrt{\left(2\bar{n}+1\right)^2-4\left|M\right|^2}$, $\Sigma\left(\bar{\alpha},\bar{\alpha}^*\right)$ is defined as

$$\Sigma\left(\bar{\alpha},\bar{\alpha}^*\right)=\left(\begin{array}{cc}\bar{\alpha} & \bar{\alpha}^*\end{array}\right)\sigma_\infty\left(\begin{array}{c}\bar{\alpha}\\ \bar{\alpha}^*\end{array}\right), \tag{36}$$

$$\sigma_\infty=\left(\begin{array}{cc}M^* & \bar{n}+\frac{1}{2}\\ \bar{n}+\frac{1}{2} & M\end{array}\right).$$

Noting the differential expression of Wigner function Eq.(30), we can finally obtain

$$W(\alpha,t)=W_r(\alpha,t)F_n(\alpha,t), \tag{37}$$

where $W_r(\alpha,t)$ is the evolution of Wigner function of squeezed vacuum in phase sensitive resevoire, and $F_n(\alpha,t)$ is a non-Gaussian item due to the presence of Hermite excitation,

$$W_r(\alpha,t)=\frac{\mu_\infty e^{-P}}{\pi\sqrt{D}}e^{\frac{1}{TD}\left(2R_1R_2R_2^*-R_3R_2^{*2}-R_2^2R_3^*\right)}, \tag{38}$$

$$F_n(\alpha,t)=\sum_{l=0}^{n}\frac{\left[n!\right]^2\left(-G_1\right)^l\left|G_2\right|^{n-l}}{l!\left[(n-l)!\right]^2} \times N_{\mu,\nu}^2\left|H_{n-l}\left(\frac{G_3}{2i\sqrt{G_2}}\right)\right|^2, \tag{39}$$

and $D=R_1^2-\left|R_3\right|^2$,

$$\begin{aligned}P&=\frac{2\mu_\infty^2}{T}\left[\left(2\bar{n}+1\right)\left|\alpha\right|^2+M\alpha^{*2}+M^*\alpha^2\right],\\ R_1&=\left(1+2\bar{n}\right)\mu_\infty^2e^{-2(t\kappa)}+T\cosh 2r,\\ R_2&=\mu_\infty^2\left(\alpha^*+2\bar{n}\alpha^*+2\alpha M^*\right)e^{-\kappa t},\\ R_3&=2\mu_\infty^2M^*e^{-2(t\kappa)}+T\sinh 2r,\end{aligned} \tag{40}$$

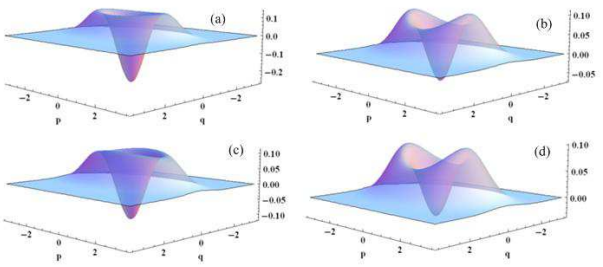

FIG. 8: (Color online) The evolution of Wigner function distribution in phase space with $n = 1$, $r = 0.3$. (a) $\kappa t = 0.01$, $M = 0.1$, $\bar{n} = 1$; (b) $\kappa t = 0.08$, $M = 0.1$, $\bar{n} = 1$; (c) $\kappa t = 0.08$, $M = 1$, $\bar{n} = 1$; (d) $\kappa t = 0.08$, $M = 0.1$, $\bar{n} = 1.5$;

as well as

$$G_1 = 4\nu_1^2 \left\{1 + \frac{T}{D}\left[(R_3 + R_3^*)\sinh 2r - 2R_1\cosh 2r\right]\right\},$$
$$G_2 = 2\mu_1\nu_1 - 1 + \frac{2T\nu_1^2}{D}\left\{2R_1\sinh 2r - (R_3 - R_3^* + (R_3 + R_3^*)\cosh 2r)\right\},$$
$$G_3 = \frac{4\nu_1}{D}R_1\left(R_2^*\sinh r + R_2\cosh r\right) - \frac{4\nu_1}{D}\left(R_2^*R_3\cosh r + R_3^*R_2\sinh r\right). \quad (41)$$

In partciular, at the center of phase space $\alpha = 0$, we have $R_2 = 0, P = 0, G_3 = 0$. Thus for the case of $n = 1$, we can get $W(\alpha, t) \propto -G_1$. Thus the existence of negative volume of WF is determined by $G_1 > 0$, which leads to

$$\kappa t < \kappa t_c = \frac{1}{2}\ln\left(\mu_\infty + 1\right), \quad (42)$$

which is independent of squeezing parameter r. It is easy to see that for any M ranging from 0 to $\bar{n}(\bar{n}+1)$,

$$\frac{1}{2}\ln\left(\frac{2\bar{n}+2}{2\bar{n}+1}\right) \leqslant \frac{1}{2}\ln\left(\mu_\infty + 1\right) \leqslant \frac{1}{2}\ln 2, \quad (43)$$

which indicates that the characteristic time of decoherence of single-photon added squeezed vacuum state in phase sensitive reservoirs is larger than that in the thermal enviornment and smaller than that in photon-loss channel.

In order to measure the degree of nonclassicality for the evoluted state, we consider the negative area and the nagative volume in phase space. As shown in Fig. 8, it is shown that the nagative area gradually dissapears with the increasemenet of $\bar{n}$, κt, while increases with parameter M. To clearly see the effects of the decoherence and parameter M on the nonclassical properties, the evolutions of negative volume with time and squeezing parameter M are plotted in Fig.9 for given $n = 1$, $r = 0.3$ and $\bar{n} = 0.5$. From Fig.9(a) one can see that the nagative volume monotonically diminnishes with κt, and there is

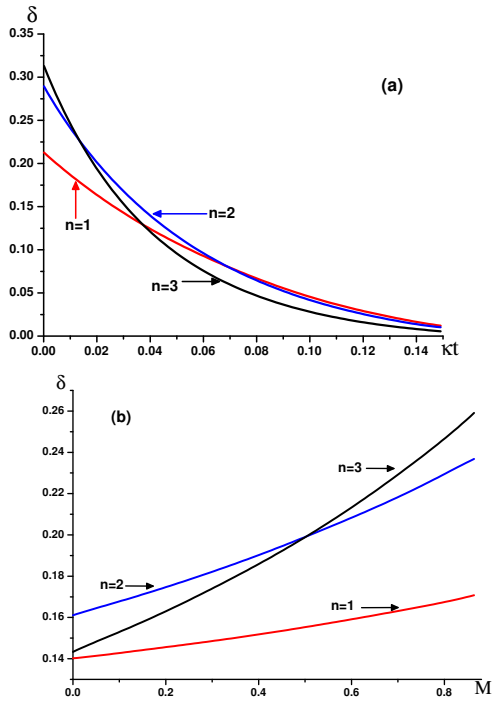

FIG. 9: (Color online) Evolution of Negative volume of Wigner function as a function of (a) κt with $M = 0.1$; (b) M with $\kappa t = 0.03$ for several different $n = 1, 2, 3$, and $r = 0.3$, $\bar{n} = 0.5$, as well as μ=ν=$1/\sqrt{2}$.

a more rapid attenuation for a big n than a small one; this leads to a smaller negative volume for a big n than a small one when κt ecseeds a certain value. From this point, one can draw a conclusion that single-photon subtraction/addition SV present a more strongger roboustness against the reservoirs than a higher-order photon subtraction/addition which could have a bigger negative volume at initial time. From Fig.9(b), it is shown that the parameter M can be used to enhance the nonclassicality of quantum state in a phase-sensitive reservoirs. Specially speaking, the negative volume increases monotonically with M. The optimal volume appears at the the maximum value of $|M|^2 = \bar{n}(\bar{n}+1)$, which inreases with n, as expected.

VI. CONCLUSIONS

In this paper, we have introduced a new non-Gaussian state, which is generated by applying Hermite-polynomial excitation on squeezed vacuum. Single-photon addition/subtraction and Hermite polynomial's addition/subtraction can be seen as its three special cases. Its normalized factor is found to be a Legendre polynomial. Then we have investigated its nonclassicality according to the Mandel's Q parameter, second-order correlation function, photon-number distribution, squeezing effects and the negativity of WF in phase

space. It is shown that all these nonclassical properties can be obviously improved by the HPS operation and can be remarkably modulated by superposition parameters μ and ν. The degree of squeezing of the HPS-SV increases with r. In particular, comparing with the SV, an observable improvement of squeezing effect can be achieved by Hermite photon-subtraction operation $H_2(a)$ and the coherent superposition operation ($H_2\left(a+a^{\dagger}\right)$) in a small region ($r \lesssim 0.6$) and a large region, respectively.

In addition, the numerical calculation of negative volume δ of WF showed that δ increases with the order n for $r \lesssim 0.45$ and decreases with r. It is interesting to notice that the negative volume δ is given $\delta = 2/\sqrt{e}-1 \approx 0.2131$ independent of μ and ν, as well as r. For high-order excitation ($n \geqslant 2$), the negative volume can be optimized by modulating parameters ν ($\mu = \sqrt{1-\nu^2}$) and n for a given r. It is found that the negative volume δ may increase with n and decrease with r when ν exceeds a certain threshold. In particular, the optimal value of δ can be obtained in a bigger region of ν ($1 > \nu \gtrsim 0.41$) not at $\nu = 0$ or $\nu = 1$. This implies that the effects of the coherent operation $H_n(\mu a + \nu a^{\dagger})$ with higher order $n \geqslant 2$ are prominent than those of the mere photon subtraction $H_n(\nu a^{\dagger})$ and the addition $H_n(\nu a^{\dagger})$ particularly in the larger region of parameter ν, whereas the optimal operation is not the photon subtraction or the photon addition in this region, which is a new result.

Furthermore, we have considered the decoherence effects of the HPS-SV in phase-sensitive reservoirs according to the analitically derived WF distribution. It is shown that the negative area and volume diminish gradually with the evolution of time and dissapear eventually. However, the negative volume of the HPS-SV with higher order excitation decays more rapidly with time, which implies that single-photon subtraction/addition SV has a more strongger roboustness than a higher-order photon subtraction/addition although the latter has a bigger negative volume at initial time. In addition, the parameter M describing the squeezing characteristic of reservoirs can be effectively used to enhance the nonclassicality.

Acknowledgments: Project supported by the National Natural Science Foundation of China (Grant No.11264018), the Natural Science Foundation of Jiangxi Province of China (Grant No. 20132BAB212006), and the Research Foundation of the Education Department of Jiangxi Province of China (no GJJ14274) as well as Degree and postgraduate education teaching reform project of jiangxi province(No. JXYJG-2013-027).

[1] D. Bouwmeester, A. Ekert, and A. Zeilinger, The Physics of Quantum Information (Springer-Verlag, 2000).

[2] G. S. Agarwal, K. Tara, "Nonclassical properties of states generated by the excitation on a coherent state," Phys. Rev. A 43, 492 (1991).

[3] P. Marek, H. Jeong, and M. S. Kim, "Generating "squeezed" superpositions of coherent states using photon addition and subtraction," Phys. Rev. A 78, 063811 (2008).

[4] M. S. Kim, "Recent developments in photon-level operations on travelling light fields," J. Phys. B 41, 133001–133018 (2008).

[5] S. Y. Lee,S. W. Ji and C. W. Lee, "Increasing and decreasing entanglement characteristics for continuous variables by local photon subtraction," Phys. Rev. A 87, 052321 (2013).

[6] Y. Yang and F. L. Li, "Entanglement properties of non-Gaussian resources generated via photon subtraction and addition and continuous-variable quantum-teleportation improvement", Phys. Rev. A 80, 022315 (2009).

[7] S. Olivares, M. G. A. Paris, and R. Bonifacio, "Teleportation improvement by inconclusive photon subtraction," Phys. Rev. A 67, 032314–032318 (2003).

[8] P. T. Cochrane, T. C. Ralph, and G. J. Milburn, "Teleportation improvement by condition measurements on the two-mode squeezed vacuum," Phys. Rev. A 65, 062306–062311 (2002).

[9] A. Kitagawa, M. Takeoka, M. Sasaki, and A. Chefles, "Entanglement evaluation of non-Gaussian states generated by photon subtraction from squeezed states," Phys. Rev. A 73, 042310-042321 (2006).

[10] S. L. Zhang and P. van Loock, "Local Gaussian operations can enhance continuous-variable entanglement distillation," Phys. Rev. A 84, 062309 (2011).

[11] S. L. Zhang, Y. Dong, X. B. Zou, B. S. Shi, and G. C. Guo, "Continuous-variable-entanglement distillation with photon addition," Phys. Rev. A 88, 032324 (2013).

[12] J. Fiurasek, "Improving entanglement concentration of Gaussian states by local displacements," Phys. Rev. A 84, 012335 (2011).

[13] C. Navarrete-Benlloch, R. Garcia-Patron, J. H. Shapiro, and N. J. Cerf, "Enhancing quantum entanglement by photon addition and subtraction," Phys. Rev. A 86, 012328 (2012).

[14] R. Roman-Ancheyta, C. Gonzalez Gutierrez, and J. Recamier, "Photon-added nonlinear coherent states for a one-mode field in a Kerr medium," 31, 38-44 (2014).

[15] A. Zavatta, S. Viciani, and M. Bellini, "Quantum-to-classical transition with single-photon-added coherent states of light," Science 306, 660–662 (2004).

[16] L. Y. Hu and H.-Y. Fan, "Statistical properties of photon-added coherent state in a dissipative channel," Phys. Scr. 79, 035004 (2009).

[17] A. Ourjoumtsev, A. Dantan, R. Tualle-Brouri, and Ph. Grangier, "Increasing entanglement between Gaussian states by coherent photon subtraction," Phys. Rev. Lett. 98, 030502 (2007).

[18] L. Y. Hu, Z. M. Zhang, "Statistical properties of coherent photon-added two-mode squeezed vacuum and its inseparability," J. Opt. Soc. Am. B 30, 286518–529 (2013).

[19] S. Y. Lee and H. Nha, "Quantum state engineering by a coherent superposition of photon subtraction and addition," Phys. Rev. A 82, 053812-1-7 (2010)

[20] S. Y. Lee, S. W. Ji, H. J. Kim, and H. Nha, "Enhancing

quantum entanglement for continuous variables by a coherent superposition of photon subtraction and addition," Phys. Rev. A 84, 012302-1-6 (2011).
[21] J. Fiurasek, "Conditional generation of N-photon entangled states of light," Phys. Rev. A 65, 053818 (2002).
[22] P. Kok, H. Lee, and J. P. Dowling, "Creation of large-photonnumber path entanglement conditioned on photodetection," Phys. Rev. A 65, 052104 (2002).
[23] S. Y. Lee and H. Nha, "Second-order superposition operations via Hong–Ou–Mandel interference," Phys. Rev. A 85, 043816 (2012).
[24] G. P. Zhang, K. M. Zheng, S. Y. Liu, and L. Y. Hu, "Statistical properties of coherent photon-subtracted two-mode squeezed vacuum and its application in quantum teleportation," Chin. Phys. B 23, 050301 (2014).
[25] L. Y. Hu, H. L. Zhang, Y. Q, Hu, and Z. M. Zhang, "Enhancing entanglement of entangled coherent states by single-mode coherent superposition of photon subtraction and addition," OPTIK 125, 61-63 (2014).
[26] J. A. Bergou, M. Hillery and D. Yu, "Minimum uncertainty states for amplitude-squared squeezing: Hermite polynomial states," Phys. Rev. A 43, 515 (1991).
[27] H. Y. Fan, X Ye, "Hermite polynomial states in two-mode Fock space," Phys. Lett. A 175, 387-390 (1993).
[28] G. Ren, J. M. Du, H. J. Yu and Y. J. Xu, "Nonclassical properties of Hermite polynomial's coherent state," J. Opt. Soc. Am. B, 29, 3412-3418 (2012).
[29] M. O. Scully, M. S. Zubairy, Quantum optics, Cambridge University Press (1997).
[30] L. Y. Hu, X. X. Xu, Z. S. Wang, and X. F. Xu, "Photon-subtracted squeezed thermal state: Nonclassicality and decoherence," Phys. Rev. A 82, 043842 (2010).
[31] L. Mandel, E. Wolf, Optical Coherence and Quantum Optics, Cambridge University Press, Cambridge (1955).
[32] D. F. Walls and G. J. Milburn, Quantum Optics, Springer-Verlag, (1995).
[33] R. J. Glauber, "Coherent and incoherent states of the radiation field," Phys. Rev. 131, 2766–2788 (1963).
[34] J. R. Klauder and B. S. Skargerstam, Coherent States, (*World Scientific*, Singapore 1985)
[35] H. Y. Fan, Representation and Transformation Theory in Quantum Mechanics, Shanghai: Shanghai Scientific and Technical Publisher, (1997).
[36] C. K. Hong and L. Mandel, "Generation of higher-order squeezing of quantum electromagnetic fields," Phys. Rev. A **32**, 974–982 (1985).
[37] J. Lee, J. Kim, and H. Nha, "Demonstrating higher-order nonclassical effects by photon-added classical states: realistic schemes," J. Opt. Soc. Am. B **26**, 1363–1369 (2009).
[38] Hong-yi Fan, "Newton-Leibniz integration for ket-bra operators in quantum mechanics (IV) - integrations within Weyl ordered product of operators and their applications," Ann. Phys. (NY) 323, 500-26 (2008).
[39] H. Y. Fan and H. R. Zaidi, "Application of IWOP technique to the generalized Weyl correspondence," Phys. Lett. A 124, 303–307 (1987).
[40] A. Kenfack, K. Zyczkowski, "Negativity of the Wigner function as an indicator of nonclassicality," J. Opt. B: Quantum and Semiclassical Optics 6, 396-404 (2004).
[41] C. W. Gardiner and P. Zoller, *Quantum Noise* (Springer Berlin, 2000).
[42] L. Y. Hu, Q. Wang, Z. S. Wang, and X. X. Xu, "Kraus Operator-Sum Representation and Time Evolution of Distribution Functions in Phase-Sensitive Reservoirs," Int. J. Theor. Phys. 51, 331–349 (2012).